Earth Planet. Sci. Lett. 669 (2025) 119592

Contents lists available at ScienceDirect

Earth and Planetary Science Letters

journal homepage: www.elsevier.com/locate/epsl

The age and early evolution of the Moon revealed by the Rb-Sr systematics of lunar ferroan anorthosites

Jonas M. Schneider [a,b,*], Thorsten Kleine [a]

[a] Max Planck Institute for Solar System Research, Justus-von-Liebig-Weg 3, 37077 Göttingen, Germany
[b] GEOMAR Helmholtz Center for Ocean Research Kiel, Wischhofstraße 1-3, 24148 Kiel, Germany

ARTICLE INFO

Editor: Dr O Mousis

Keywords:
Age of the Moon
Lunar Chronology
Rb-Sr isotopes
Ferroan Anorthosites

ABSTRACT

The formation of the Moon by a giant impact of an object called Theia onto proto-Earth marks the end of the main stage of Earth's accretion. However, the timing of this event is controversial, with estimates ranging between ~50 and ~220 million years (Ma) after solar system formation. The ^{87}Rb-^{87}Sr system has the potential to resolve this debate, as formation of the Moon resulted in strong fractionation of rubidium from strontium. To better determine the initial ^{87}Sr/^{86}Sr of the Moon, we obtained Rb-Sr isotope data for several lunar ferroan anorthosites, which define an initial ^{87}Sr/^{86}Sr of 0.6990608±0.0000005 (2 s.e.) at 4.360±0.003 Ga. Modeling the pre-giant impact Rb-Sr isotopic evolution of Theia and the proto-Earth reveals that while in the canonical giant impact model no Rb-Sr model age can be determined, all other current impact models yield a Moon formation age of 4.502±0.020 Ga, or 65±20 Ma after solar system formation. When compared to the chronology of lunar samples, this age implies that solidication of the lunar magma ocean took ~70 Ma, and that the Moon underwent a global re-melting event ~150 Ma after its formation.

1. Introduction

The Moon is thought to have formed as the result of a giant impact of an object called 'Theia' with proto-Earth near the end of Earth's accretion (Canup and Asphaug, 2001). Despite its importance for determining the timescale of Earth's formation, until now the age of the Moon has not been determined precisely, and current estimates range from ~4.52 to ~4.35 billion years ago (Ga), or ~50 to ~220 million years (Ma) after solar system formation (Barboni et al., 2017; Borg et al., 2019, 2011; Bottke et al., 2015; Dauphas et al., 2025; Greer et al., 2023; Halliday, 2008; Jacobson et al., 2014; Maurice et al., 2020; Nemchin et al., 2009; Woo et al., 2024). The most common approach to determine the Moon's formation time is by dating the different rock types assumed to have crystallized from the lunar magma ocean (LMO), which had formed as a result of the energy released by the giant impact (Smith et al., 1970; Warren, 1985). Solidification of the LMO led to chemical differentiation of the Moon through the separation of dense mafic cumulates from buoyant plagioclase-rich cumulates, which formed the ferroan anorthosites (FAN) that dominate the lunar crust (Elardo et al., 2011; Snyder et al., 1992; Warren, 1985; Wood et al., 1970). The end of LMO crystallization is commonly associated with the formation of a residual liquid referred to as KREEP [for potassium (K), rare earth elements (REE), and phosphorus(P); Warren and Wasson, 1979], and the crystallization of the Mg-suite, which represent melts intruded into the earlier-formed anorthositic crust (Borg and Carlson, 2023; Zhang et al., 2021a).

Formation ages for early- and late-formed products of the LMO based on the analyses of lunar whole-rock samples consistently return ages of ~4.35 Ga (see summary in Borg and Carlson, 2023); these include crystallization ages of FANs, which are thought to have formed soon after the Moon's formation (Borg et al., 2011), and model ages for KREEP, which mark the end of LMO crystallization (Gaffney and Borg, 2014). This consistency of ages has been interpreted to indicate rapid LMO crystallization at ~4.35 Ga, which in turn would imply that the Moon formed at around this time, i.e., ~220 Ma after solar system formation. However, the ^{176}Lu-^{176}Hf isotope systematics of lunar zircons have been used to determine an older KREEP source formation age of 4.51±0.01 Ga (Barboni et al., 2017), which was recently revised to 4.429±0.076 Ga (Dauphas et al., 2025). Although this age marginally overlaps with the aforementioned ~4.35 Ga age peak, there also are lunar zircons having crystallization ages of ~4.41–4.45 Ga (Grange et al., 2011; Greer et al., 2023; Meyer et al., 1996; Nemchin et al., 2009,

* Corresponding author.
E-mail address: joschneider@geomar.de (J.M. Schneider).

https://doi.org/10.1016/j.epsl.2025.119592
Received 19 June 2025; Received in revised form 8 August 2025; Accepted 12 August 2025

2008; Taylor et al., 2009; Zhang et al., 2021b), which together have been interpreted to indicate that the Moon formed earlier than ~4.45 Ga. In this case, the aforementioned prevalence of ~4.35 Ga lunar whole-rock ages would have to record a large, potentially global secondary magmatic event unrelated to the original crystallization of the LMO (Borg et al., 2015; Borg and Carlson, 2023; Gaffney and Borg, 2014). It has been suggested that re-melting of large parts of the Moon is related to formation of the South-Pole Aitken basin (Barboni et al., 2024) or to tidal heating during the Moon's passage through the Laplace Plane Transition (Nimmo et al., 2024). Either way, the discrepancy between lunar whole-rock and zircon ages combined with the possibility that later re-melting of the Moon occurred highlight the difficulty in using ages of LMO products to determine the Moon's formation time.

An alternative way of dating the formation of the Moon is to determine the time of a major chemical fractionation in the Moon that is closely associated with the giant impact. The Moon is strongly depleted in moderately volatile elements [elements with condensation temperatures lower than Mg and Si but higher than FeS; Wolf and Anders (1980)], which has been attributed to incomplete condensation of the proto-Moon (Canup et al., 2015; Lock et al., 2018), volatile loss from the molten Moon (Charnoz et al., 2021), or mixing of volatile-poor and -rich materials during Moon formation (Mezger et al., 2021). All these interpretations imply that the Moon's moderately volatile element depletion has been established during or soon after the Moon's formation. Consequently, because Rb is moderately volatile, while Sr is refractory, the ^{87}Rb-^{87}Sr isotope system has the potential to date the formation of the Moon (Halliday, 2008). To calculate a Rb-Sr age of the Moon, prior studies used Rb-Sr isotope data of a single FAN sample (FAN 60025) to define the initial Sr isotope composition of the Moon and assumed that there was efficient post-giant impact isotopic equilibration between the Earth and the Moon, such that the initial Sr isotope composition of the Moon also reflects that of Earth (Halliday, 2008; Mezger et al., 2021; Yobregat et al., 2024). On this basis, Rb-Sr ages of 4.48±0.02 Ga (Halliday, 2008), 4.507±0.015 Ga (Mezger et al., 2021), and >4.488 Ga (Yobregat et al., 2024) have been reported. There are, however, two major sources of uncertainty in these Rb-Sr ages. First, it is unclear as to whether a single sample accurately records the initial Sr isotopic composition of the Moon. For instance, some studies argued that FANs formed over an extended period of time (Michaut and Neufeld, 2022), in which case different FANs may have different initial Sr isotopic compositions and FANs with less radiogenic Sr isotope compositions than FAN 60025 may exist. Thus, the determination of the Moon's initial Sr isotopic composition should rely on Rb-Sr data for a larger suite of FANs. Second, although Earth-Moon isotopic equilibration is often invoked as an explanation for the indistinguishable isotopic compositions of the Earth and Moon (Pahlevan and Stevenson, 2007), it is unknown as to whether any Sr isotope heterogeneity between proto-Earth and Theia has been completely erased during or immediately after the Moon's formation (Borg et al., 2022). As such, it is important to assess under which circumstances the Rb-Sr system constrains the age of the Moon without the assumption of Earth-Moon equilibration.

To more rigorously explore the utility of the Rb-Sr system to date the Moon, we obtained high-precision Rb-Sr data for several FANs to better define the initial Sr isotope composition of the Moon. We use the new data to model the Rb-Sr isotope evolution of the Earth-Moon system within the framework of current lunar formation models, including models that do not rely on Earth-Moon equilibration, and show that the Rb-Sr age constraints can help reconciling some of the existing discrepancies in lunar chronology.

2. Samples and methods

2.1. Samples and sample preparation

Eight FANs from the Apollo 15 and 16 missions were selected: 15415, 60015, 60025, 61015, 62255, 65315, 65325, and 67075. Some of these samples have previously been investigated for their Rb-Sr systematics (see Table S1 for references), but except for sample 60025, the precision of the Sr isotope data achievable at the time of these earlier studies was about one of order magnitude worse compared to current techniques. The sample selection was guided by (*i*) the presence of large anorthite crystals, which more readily allows separating intact mineral grains, (*ii*) low reported Rb concentrations, which is essential for precisely determining a sample's initial ^{87}Sr/^{86}Sr, and (*iii*) low reported ^{87}Sr/^{86}Sr values and/or other evidence for old formation ages (Table S1). In total, 14 different fractions from these samples were analyzed: ten plagioclase separates ('-p'), three bulk samples ('-b'), one residue after hand picking ('-r'), and one sieved fine fraction ('-f'; <125 μm).

Between 50 and 200 mg of FAN samples were crushed in an agate mortar and pure plagioclase grains were handpicked under a binocular. Where necessary, samples were passed through a 125 μm sieve to obtain intact grains. Relatively pure anorthites were identified as translucent grains with plain surfaces and no visible dark patches or inclusions (Fig. S1). Altogether, ten plagioclase separates ('-p'), three bulk samples ('-b'), one residue after hand picking ('-r'), and one sieved fines fraction ('-f'; > 125μm) were measured. After weighing, the samples were cleaned with Milli-Q water in an ultrasonic bath to remove any surface contamination. The use of any acid for washing was avoided, to not risk Rb-Sr fractionation through leaching. Analyses of the wash fractions show tens to hundreds of picograms Rb in some fractions, highlighting the importance of removing the surface contamination. While it is difficult to demonstrate that all surface Rb has been removed by this method, the good linear correlation of the data in the Rb-Sr isochron diagram and the observation that most samples define a common initial ^{87}Sr/^{86}Sr (see below) provides strong evidence that any remaining Rb contamination was minor to absent.

2.2. Chemical separation

After washing, the samples were digested in pre-cleaned Teflon beakers using double distilled HF-HNO_3 (2:1) at 140°C for 2–3 days, followed by dissolution in *aqua regia* at 140°C for 2 days. Subsequently, the samples were dried, redissolved in 0.5 ml 6 M HCl and dried again, and then re-dissolved in 2 ml 2.5 M HCl. Depending on the amount of sample available, some of the samples were split into two aliquots. One aliquot was spiked with a ^{85}Rb-^{84}Sr tracer for the determination of Rb and Sr concentrations by isotope dilution (ID-aliquot). The other aliquot (IC-aliquot) was used solely for measuring Sr isotopic compositions. This procedure allows direct comparison of the Sr isotope results for unspiked and spiked samples (for which the spike was subtracted), which for all samples are in excellent agreement (Fig. S3). For samples for which less material was available, no IC-aliquot was taken, and the entire sample was mixed with an appropriate amount of the ^{85}Rb-^{84}Sr spike.

After aliquoting and spiking, samples were loaded onto quartz glass columns filled with 5 ml cation exchange resin (BioRad AG-50W-X2, 200–400 mesh), and Rb and Sr were eluted sequentially using 2.5 M HCl (Nebel et al., 2005). The Rb and Sr cuts were dried, re-dissolved in concentrated HNO_3, and diluted to 0.25 ml 5 M HNO_3. These solutions were loaded onto homemade microcolumns filled with 100 μl Eichrom Sr-spec-B resin, and Rb was eluted using 1.2 ml 5 M HNO_3, followed by Sr, which was eluted with 1.7 ml Milli-Q water. This procedure resulted in sufficiently clean Rb-ID, Sr-ID, and Sr-IC cuts for isotope measurements.

Given the low Rb but high Sr contents of the samples, any blank contribution is expected to be negligible for Sr, but can be substantial for Rb. Thus, Rb blanks were carefully monitored throughout this study, and for each sample a Rb blank was processed through the entire digestion and chemical procedure. Total procedural Rb blanks were between 3 and 16 pg (n = 12, 3/4 < 10 pg), resulting in < 5 % Rb blank

contribution for most of the samples [except samples 65315-p (29 %) and 65325-p (8 %)]. Uncertainties introduced by the blank correction are propagated in the final uncertainty of the $^{87}Rb/^{86}Sr$ ratios reported in Table 1. Total procedural blanks for Sr were between 5 and 16 pg (n = 2) and were negligible.

2.3. Isotope measurements

All isotope measurements were performed using the Thermo Fisher Triton XT at the Max Plank Institute for Solar System Research (MPS). For the Rb-ID measurements, ~0.5 ng Rb was mixed with a Ta_2O_5 activator, loaded onto outgassed Re filaments, and the measurements were performed at a filament temperature of 600–700°C for 40 cycles in static mode. Interferences from ^{87}Sr on ^{87}Rb were monitored by also measuring the ion beam on ^{88}Sr, but no ^{88}Sr signal above baseline was observed. Instrumental mass fractionation was corrected using measurements of the NIST 984 Rb standard in the same session, and assuming a natural $^{87}Rb/^{85}Rb$ ratio of 0.38554 (Nebel et al. 2005). Repeated measurements of this standard yielded an external uncertainty on measured $^{87}Rb/^{85}Rb$ ratios of ±0.5 % (2 s.d.). Owing to the low Rb contents of the samples, the largest contributor to the uncertainty on the Rb concentrations is the Rb blank correction, which lead to final uncertainties on the $^{87}Rb/^{86}Sr$ ratios of up to ~5 % (2 s.d.). However, because of the low $^{87}Rb/^{86}Sr$ ratios of the samples of this study, this uncertainty is inconsequential for the interpretation of the Rb-Sr isotopic data.

The Sr isotope measurements of the Sr-IC and Sr-ID aliquots used a three-line multi-dynamic data acquisition scheme described previously (Hans et al., 2013; Schneider and Kleine, 2024). Each measurement typically consisted of 300–600 cycles and the final $^{87}Sr/^{86}Sr$ is obtained from the $^{87}Sr/^{86}Sr$ measured in each line corrected for mass fractionation relative to $^{86}Sr/^{88}Sr = 0.1194$ using the exponential law and the $^{88}Sr/^{86}Sr$ measured in two of the lines (for details see Schneider and Kleine, 2024). Repeated measurements of the NIST SRM987 Sr standard during the course of this study yielded $^{87}Sr/^{86}Sr = 0.710245\pm0.000005$ (2 s.d., n = 43). If possible, samples were measured multiple times and the errors are reported as 2s.e. for $n \geq 4$ or twice the standard deviation (2 s.d.) of the standards measured within the same session for $n < 4$.

3. Results

The Rb-Sr results are summarized in Table 1 and plotted on Fig. 1. The plagioclase fractions have Rb contents below ~50 ppb and correspondingly low $^{87}Rb/^{86}Sr$ ratios smaller than 0.0009. Only plagioclase from sample 67075 has a slightly higher Rb content and due to its somewhat lower Sr content has the highest $^{87}Rb/^{86}Sr$ ratio of the plagioclase fractions analyzed in this study. All of the three bulk fractions and the fines fraction have higher $^{87}Rb/^{86}Sr$ ratios than the plagioclase fractions of the same samples, but two of the bulk fractions (from samples 65315 and 65325) have $^{87}Rb/^{86}Sr$ ratios within the overall range of values observed among the plagioclase fraction. These observations indicate that the Rb in these samples is predominantly located at grain boundaries between the plagioclase grains and in small melt patches. This highlights the importance of analyzing pure plagioclase fractions for reliably determining the initial $^{87}Sr/^{86}Sr$ ratios of the samples. As we will show below, all but one of the analyzed plagioclase fractions have sufficiently low $^{87}Rb/^{86}Sr$ ratios that allow the reliable determination of their initial $^{87}Sr/^{86}Sr$ ratios.

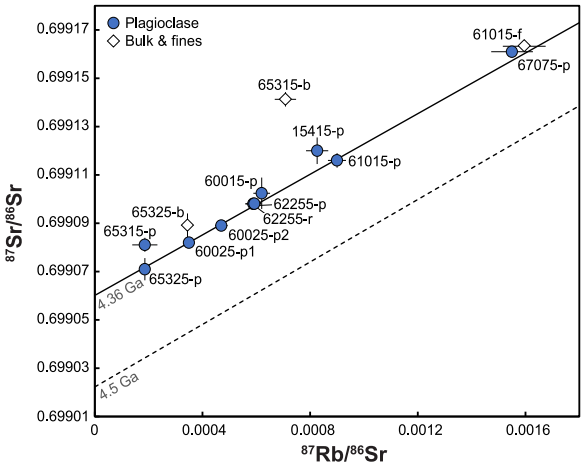

Fig. 1. Rb-Sr isochron diagram for FANs of this study. Reference isochrons for 4.36 Ga and 4.5 Ga are calculated using a bulk lunar $^{87}Rb/^{86}Sr = 0.018$, and assuming the initial $^{87}Sr/^{86}Sr$ of FAN 60025 at its age of 4.36 Ga.

The $^{87}Sr/^{86}Sr$ ratios of the FAN samples are broadly correlated with their $^{87}Rb/^{86}Sr$, and the plagioclase fraction of six samples (60015, 60025, 61015, 62255, 65325, 67075) plot on a single reference isochron (Fig. 1). Linear regression of the Rb-Sr data for these samples yields an age of 4.5±0.5 Ga (MSWD = 0.26) but a precise initial $^{87}Sr/^{86}Sr$ of 0.6990590±0.0000038 (95 % conf.). The low precision of this age reflects the limited spread in and overall low $^{87}Rb/^{86}Sr$ ratios among these samples, which in turn allow precise determination of their initial $^{87}Sr/^{86}Sr$ ratios. The fines fraction of sample 61015 plots within uncertainty on the isochron, while the three bulk fractions and two plagioclase fractions (65315, 15415) plot above the isochron.

The only FAN of this study that has previously been analyzed for its Rb-Sr systematics is sample 60025 (Borg et al., 2011; Carlson and Lugmair, 1988; Yobregat et al., 2024). The $^{87}Rb/^{86}Sr$ and $^{87}Sr/^{86}Sr$ ratios obtained for plagioclase fractions from 60025 in this study are in good

Table 1
Rb-Sr isotopic data for ferroan anorthosites.

Sample	Type[a]	Weight (mg)	Rb (ppm)	Sr (ppm)	$^{87}Rb/^{86}Sr$[a]	n	$^{87}Sr/^{86}Sr$[a]
15415	Plag.	30.0	0.045±0.002	157±2	0.00083±4	2	0.699120±6
60015	Plag.	18.0	0.034±0.002	161±2	0.00062±3	1	0.699102±7
60025	Plag.	16.9	0.022±0.001	183±2	0.00035±2	5	0.699082±2
60025	Plag.	15.9	0.030±0.002	188±2	0.00047±2	3	0.699089±2
61015	Plag.	6.0	0.051±0.003	169±2	0.00090±5	1	0.699117±2
61015	Bulk rock	27.4	0.233±0.012	193±2	0.00350±18	4	0.699273±2
61015	Fines	29.3	0.103±0.005	185±2	0.00160±8	4	0.699163±2
62255	Plag.	15.2	0.032±0.002	157±2	0.00059±4	1	0.699098±2
62255	Plag. residue	16.0	0.033±0.002	157±2	0.00059±3	4	0.699098±1
65315	Plag.	6.2	0.009±0.001	140±1	0.00019±6	2	0.699081±3
65315	Bulk rock	19.5	0.030±0.002	123±1	0.00071±4	4	0.699141±3
65325	Plag.	9.4	0.010±0.001	184±2	0.00019±2	2	0.699071±5
65325	Bulk rock	24.8	0.015±0.001	166±2	0.00034±2	3	0.699089±5
67075	Plag.	13.5	0.067±0.003	125±1	0.00155±8	4	0.699161±2

[a] Uncertainties on $^{87}Rb/^{86}Sr$ and $^{87}Sr/^{86}Sr$ refer to the last significant digits and for $^{87}Sr/^{86}Sr$ are given as 2 s.e. for $n \geq 4$ or as the 2 s.d. of the SRM 987 measurements within the same session for $n < 4$. $^{87}Sr/^{86}Sr$ are normalized to $^{87}Sr/^{86}Sr = 0.710245$ for SRM 987.

agreement with the results of these prior studies (Fig. S2). In detail our results are more precise than those of two older studies on 60025 (Borg et al., 2011; Carlson and Lugmair, 1988), and similarly precise as the results of a recent study (Yobregat et al., 2024), reflecting the improved precision achievable with current mass spectrometric techniques.

4. Discussion

4.1. The initial Sr isotope composition of the Moon

The low $^{87}Rb/^{86}Sr$ of FANs allow precise measurements of their initial $^{87}Sr/^{86}Sr$, which owing to the low $^{87}Rb/^{86}Sr$ of the bulk Moon can then be used to determine the initial $^{87}Sr/^{86}Sr$ of the Moon itself. The observation that some of the samples of this study plot above the isochron defined by most of the plagioclase fractions provides evidence for some level of disturbance of the Rb-Sr system in these samples, which is most likely related to post-crystallization impact metamorphism during the intense bombardment of the lunar surface until ~3.8 Ga, the time of the late heavy bombardment (Tera et al., 1974; Wetherill, 1975). As such, the reliable determination of the initial $^{87}Sr/^{86}Sr$ ratios of FANs requires the analyses of samples with sufficiently low $^{87}Rb/^{86}Sr$ ratios such that the correction of measured $^{87}Sr/^{86}Sr$ for radiogenic ingrowth is independent of the assumed age of a sample. Considering an age difference of between 4.36 and 3.8 Ga (i.e., the difference between the crystallization age of FAN 60025 and the time of the late heavy bombardement) yields a ~10 ppm difference in age-corrected initial $^{87}Sr/^{86}Sr$ ratios for a $^{87}Rb/^{86}Sr$ ratio of 0.001. Thus, given an external reproducibility of ±5 ppm of the $^{87}Sr/^{86}Sr$ measurements, the initial $^{87}Sr/^{86}Sr$ of a sample can be determined reliably (i.e., independent of its assumed age) for samples having $^{87}Rb/^{86}Sr \leq 0.001$. This condition is met by all but one (sample 67075) of the plagioclase fractions analyzed in this study (Table 1, Fig. 1). This approach relies on the assumption that there had been no change in the $^{87}Rb/^{86}Sr$ ratios of the analyzed plagioclase fractions after 3.8 Ga. This assumption is reasonable because any post-crystallization change of the $^{87}Rb/^{86}Sr$ likely occurred during impact metamorphism (e.g., by volatilization of Rb) and, as such, should largely have happened before or during the late heavy bombardment at 3.8 Ga.

Among the FANs with sufficiently low $^{87}Rb/^{86}Sr$ is sample 60025, for which a precise absolute age of 4.360±0.003 Ga has been determined (Borg et al., 2011). Thus, for the age correction of measured $^{87}Sr/^{86}Sr$ ratios of the plagioclase fractions we use the age of FAN 60025, although as noted above, using a different age does not change the results. The initial $^{87}Sr/^{86}Sr$ ratios calculated in this manner agree with each other and define a mean initial $^{87}Sr/^{86}Sr = 0.6990608\pm0.0000005$ (2s.e., n = 7) (Table 2, Fig. 2), indistinguishable from the initial $^{87}Sr/^{86}Sr = 0.6990590\pm0.0000038$ (2s.e., n = 7) obtained from the isochron regression of these samples (Fig. 1). Two other FANs investigated in this study (65315, 15415) plot slightly above the reference isochron defined by the other samples and are, therefore, characterized by higher inferred initial $^{87}Sr/^{86}Sr$ ratios (Fig. 1). Thus, these samples either formed later than the other five FANs or their Rb-Sr systematics have been disturbed by post-crystallization processes such as for instance impact metamorphism.

Table 2
Initial $^{87}Sr/^{86}Sr$ for five FANs of this study and their corresponding model ages relative to FAN 60025.

Sample	Type	$^{87}Sr/^{86}Sr_{initial}$[a,b] (± 2s.e.)	Rb-Sr model age[c]
60015	Plag.	0.699064±7	4345±26
60025	Plag. #1	0.699060±2	4359±*17*
60025	Plag. #2	0.699060±2	*4361±8*
61015	Plag.	0.699061±2	4356±6
62255	Plag.	0.699061±1	4355±4
62255	Plag. residue	0.699061±1	*4357±5*
65325	Plag.	0.699059±5	*4362±18*
	Average	*0.6990608±5*	*4356±4*

[a] Normalized to 0.710245
[b] Error refers to last digit, and were propagated through calculation of the initial
[c] Model age assuming a bulk lunar $^{87}Rb/^{86}Sr = 0.018\pm0.006$ and $^{87}Sr/^{86}Sr = 0.699060$ at 4360 Ma

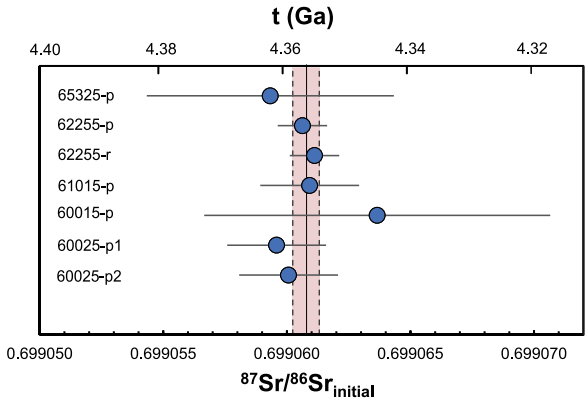

Fig. 2. Initial $^{87}Sr/^{86}Sr$ ratios and corresponding model ages for five FANs of this study. These samples are used to define the initial $^{87}Sr/^{86}Sr$ of the Moon at 4.36 Ga (Table 2).

The initial $^{87}Sr/^{86}Sr$ of FANs determined in this study is indistinguishable from that of FAN 60025 reported in prior studies, but is now more reliably determined based on several samples. More importantly, none of the samples of this study shows evidence for a less radiogenic initial $^{87}Sr/^{86}Sr$, which, given the relatively young age of FAN 60025 of ~4.36 Ga may be expected to exist. Below we first use the new Rb-Sr data to evaluate the age of the Moon and then discuss the significance of the Rb-Sr systematics of FANs in the context of lunar chronology.

4.2. Rb-Sr age of the Moon

Until now, a Rb-Sr age for the Moon has been determined by assuming efficient post-giant impact Earth-Moon equilibration, in which case the initial $^{87}Sr/^{86}Sr$ of the Moon determined based on FANs would also be the immediate post-giant impact initial $^{87}Sr/^{86}Sr$ of the Earth. However, the extent to which Earth-Moon isotopic equilibration occurred is debated (Borg and Carlson, 2023; Canup et al., 2023). This raises the question of whether a Rb-Sr model age can still be determined even when Earth-Moon equilibration did not occur. To assess under which conditions this is possible, we calculated the Rb-Sr isotopic evolution of proto-Earth and the Moon-forming impactor Theia in current formation models for the Moon. We distinguish between four different impact scenarios (for a summary see Canup et al., 2023): (*i*) the canonical impact model (Cameron and Ward, 1976; Hartmann and Davis, 1975), in which the Moon predominantly consists of material from Theia; (*ii*) models that invoke Earth-Moon isotopic equilibration (e.g., Lock et al., 2018); (*iii*) models in which the Earth and the Moon consist of similar mixtures of proto-Earth and Theia [e.g., the half Earth model (Canup, 2012)]; and (*iv*) models in which the Moon is formed mainly from proto-Earth's mantle [e.g., the fast-spinning Earth model (Cuk and Stewart, 2012)]. The last three of these models account for both the physical properties of the Moon (i.e., mass, angular momentum) and the Earth-Moon isotopic similarity, but they do so in different ways. In the half-Earth and fast-spinning Earth models, the Earth-Moon isotopic similarity results from the physical transport of material to the lunar accretion disk, while the equilibriation model assumes post-giant isotopic equilibration. Importantly, while such equilibration may have also occurred in the canonical scenario (Pahlevan and Stevenson, 2007), we here consider the original canonical model without equilibration to assess the disparate effects of equilibration versus non-equilibration on the Rb-Sr systematics.

4.2.1. Equilibrium case

Of the four aforementioned models, we start with the equilibration model because this is the model that has been used in prior Rb-Sr studies on the Moon (Halliday, 2008; Mezger et al., 2021; Yobregat et al., 2024). With the assumption of Earth-Moon isotopic equilibration, a Rb-Sr model age of the Moon can be determined by calculating the time at which a reservoir characterized by the BSE's $^{87}Rb/^{86}Sr$ ratio has evolved to the lunar $^{87}Sr/^{86}Sr$ as follows (Supplementary Information):

$$t_{Moon} \approx \frac{b\lambda t_{CAI} - d\lambda t_{FAN} + a - c}{(b-d)\lambda}$$

where the parameters are defined as follows:

$$a = \left(\frac{^{87}Sr}{^{86}Sr}\right)_{SSI},\ b = \left(\frac{^{87}Rb}{^{86}Sr}\right)_{BSE},\ c = \left(\frac{^{87}Sr}{^{86}Sr}\right)_{FAN,t},\ d = \left(\frac{^{87}Rb}{^{86}Sr}\right)_{Moon}$$

Current best estimates for parameters *a*, *b*, and *d* are summarized in Table S2. Of these parameters, the initial $^{87}Sr/^{86}Sr$ of the solar system is the most uncertain and the two most recent studies (Mezger et al., 2021; Yobregat et al., 2024) have used the value determined based on angrites, extremely volatile-depleted differentiated achondrites whose initial $^{87}Sr/^{86}Sr$ is precisely determined (Hans et al., 2013). However, these angrites formed ~4 Ma after solar system formation (Amelin, 2008; Kleine et al., 2012; Tissot et al., 2017), and so depending on when Rb loss from the angrite parent body occurred, their initial $^{87}Sr/^{86}Sr$ does not necessarily reflect the solar system initial value. This value may more directly be determined using Ca-Al-rich inclusions (CAIs), which are the oldest dated solids of the solar system. However, CAIs carry nucleosynthetic Sr isotope anomalies, as manifested in variations in the $^{84}Sr/^{86}Sr$ ratio (internally normalized to a fixed $^{88}Sr/^{86}Sr$) (Hans et al., 2013; Moynier et al., 2012; Papanastassiou and Wasserburg, 1978). Depending on whether the Sr isotope anomalies reflect the heterogeneous distribution of Sr from the *p*- (proton-capture), *s*- (slow neutron capture), or *r*-processes (rapid neutron capture), the effects on $^{87}Sr/^{86}Sr$ vary and, as such, impact the estimate of a sample's initial $^{87}Sr/^{86}Sr$. Hans et al. (2013) assumed that the ^{84}Sr anomalies in CAIs are due to variations in *r*-process Sr because the same CAIs they analyzed display *r*-process Mo isotope variations (Burkhardt et al., 2011). In this case the initial $^{87}Sr/^{86}Sr$ of CAIs requires an upward correction from the measured value of 0.698930 (re-normalized to 0.710245 for the NIST SRM 987 standard) to a value of 0.698970 (Hans et al., 2013). This higher value happens to be indistinguishable from the initial $^{87}Sr/^{86}Sr$ measured for angrite and eucrite meteorites (Hans et al., 2013), both of which show no nucleosynthetic Sr isotope anomalies (Hans et al., 2013; Schneider et al., 2023). In this case the initial $^{87}Sr/^{86}Sr$ of the angrites may indeed represent the solar system value. However, it has also been shown that some CAIs exhibit large internal $^{84}Sr/^{86}Sr$ variations accompanied by more subdued variations in $^{87}Sr/^{86}Sr$, indicating that at least some of the nucleosynthetic Sr isotope anomalies in CAIs reflect heterogeneities solely in the *p*-process nuclide ^{84}Sr (Charlier et al., 2021). These variations do not require any correction of the $^{87}Sr/^{86}Sr$ ratio, and so the upward correction of the measured initial $^{87}Sr/^{86}Sr$ of CAIs assuming that the Sr isotope anomalies solely reflect *r*-process heterogeneity may be too large. To account for this uncertainty, we use a solar system initial $^{87}Sr/^{86}Sr = 0.698950 \pm 0.000020$ (Figs. S4-S6), which covers the entire range of possible initial values from 0.698930 (i.

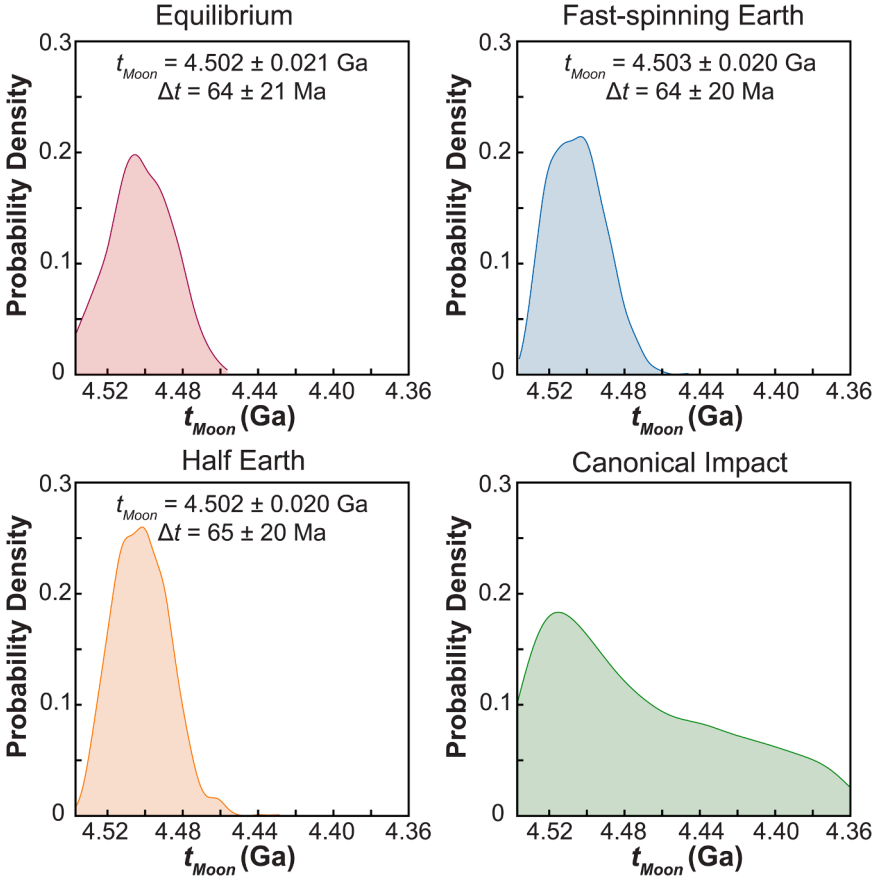

Fig. 3. Rb-Sr model ages for the time of Moon formation calculated for four different impact scenarios. No discrete peak is obtained for the canonical impact scenario, but all other scenarios provide a consistent Moon formation age of 4.502±0.020 Ga, or 65±20 Ma after solar system formation. Ages and associated errors were determined by the full-width-at-half-maximum of the peaks. The minimum age for formation of the Moon was set to 4.537 Ga, which is the earliest time possible for Moon formation as defined by the two-stage Hf-W model age of terrestrial core formation (Kleine et al., 2002; Nimmo and Kleine, 2015); the maximum age was set to 4.360±0.003 Ga as defined by the age of FAN 60025 (Borg et al., 2011).

e., the measured value which would represent the solar system initial provided the ^{84}Sr anomalies in CAIs entirely reflect *p*-process variations) to 0.698970 (i.e., the corrected CAI initial assuming that the ^{84}Sr anomalies in CAIs reflect only *r*-process variations). As shown below, the particular choice of the solar system initial $^{87}Sr/^{86}Sr$ is important for determining a Rb-Sr age of the Moon.

By randomly varying the four parameters *a, b, c*, and *d* in equation (1) within their respective error bounds (Table S2), we calculate an age of 4.502±0.021 Ga, or 65±21 Ma after solar system formation (Fig. 3). This age is broadly consistent with Rb-Sr ages of between ~50 and 90 Ma (Halliday, 2008; Mezger et al., 2021; Yobregat et al., 2024) reported in prior studies, but this consistency is partly coincidence, for two reasons (Fig. 4). First, unlike in two of these prior studies (Halliday, 2008; Mezger et al., 2021), our approach considers the Sr isotopic evolution within the Moon prior to crystallization of FANs, which results in Moon formation ages that are ~30 Ma older than the ages calculated without correcting the FAN's initial $^{87}Sr/^{86}Sr$ for radiogenic ingrowth within the Moon. This, together with the new and more precise $^{87}Sr/^{86}Sr$ determined in this study, accounts for the difference of our Rb-Sr age compared to the 87±13 Ma estimate from an earlier study (Halliday, 2008). Second, the choice of the initial $^{87}Sr/^{86}Sr$ ratio of the solar system has a similarly large effect on the calculated age (see Fig. S4-S6). Using the initial $^{87}Sr/^{86}Sr$ derived from angrite meteorites results in Rb-Sr model ages that are ~30–40 Ma older compared to ages calculated relative to the initial $^{87}Sr/^{86}Sr$ determined based on CAIs. As such, the good agreement of our Rb-Sr age compared to the 60±15 Ma age from Mezger et al. (2021) reflects that this former age should be ~30 Ma younger because the Sr isotope evolution within the Moon was not considered, but should also be ~25 Ma older because a different, higher solar system initial $^{87}Sr/^{86}Sr$ was used. A more recent study also used this higher initial $^{87}Sr/^{86}Sr$ and found a maximum Rb-Sr age of 79 or 51 Ma for the Moon, depending on the assumed $^{87}Rb/^{86}Sr$ ratio for the Moon (Yobregat et al., 2024; Fig. 4). Using the more conservative estimate for the solar system initial $^{87}Sr/^{86}Sr$ from the present study would make this age ~25 Ma younger, consistent with the Rb-Sr age of 65 ± 21 Ma we calculate. Finally, the uncertainty of the Rb-Sr age of this study is somewhat larger than uncertainties reported in most of the earlier studies, because we use a more conservative uncertainty on the initial $^{87}Sr/^{86}Sr$ of the solar system and include the Sr isotope evolution within the Moon.

4.2.2. Non-equilibrium models

Without the assumption of Earth-Moon equilibration, a Rb-Sr age cannot be calculated as outlined above, because we cannot assume *a priori* that the Earth and Moon had the same immediate post-giant impact $^{87}Sr/^{86}Sr$. To assess if a Rb-Sr age can nevertheless be determined, we calculate the $^{87}Rb/^{86}Sr$ of the Earth and the $^{87}Sr/^{86}Sr$ of the Moon (i.e., the two parameters that are well constrained) resulting from the particular mixture of proto-Earth and impactor (i.e., Theia) materials predicted in different Moon formation scenarios (Table S3). In these models, the $^{87}Rb/^{86}Sr$ ratios of proto-Earth and Theia are not known and are, therefore, assumed to be within the range of compositions observed among meteorite parent bodies (Supplementary Materials). Their corresponding $^{87}Sr/^{86}Sr$ ratios at the time of Moon formation are determined by calculating the radiogenic ingrowth since the time of solar system formation until the time of the Moon-forming impact, and using the respective $^{87}Rb/^{86}Sr$ of each body. In reality, neither proto-Earth nor Theia are expected to have evolved with a single $^{87}Rb/^{86}Sr$ until the giant impact, but since we consider the full range of plausible $^{87}Rb/^{86}Sr$ ratios for both objects, all possible Rb-Sr isotopic evolution of these bodies should be covered in these calculations ($\geq 5\times10^5$ models for each scenario). The resulting $^{87}Rb/^{86}Sr$ of the bulk silicate Earth (BSE) and $^{87}Sr/^{86}Sr$ of the Moon can then be calculated by mass balance (Supplementary Materials). We ran Rb-Sr evolution calculations for different Moon formation scenarios, where the input parameters ($^{87}Rb/^{86}Sr$ ratios of Theia and proto-Earth, size of Theia, and mass fraction of Theia in the Moon) are varied randomly according to the respective impact scenario, and the time of the giant impact is a free parameter. Models are considered successful when $^{87}Rb/^{86}Sr_{BSE} = 0.08\pm0.01$ and $^{87}Sr/^{86}Sr_{Moon}$ at time $t = 4.360\pm0.003$ Ga matches the observed $^{87}Sr/^{86}Sr$ FAN = 0.6990608±0.0000005. Thus, unlike in prior studies (Halliday, 2008; Mezger et al., 2021; Yobregat et al., 2024), these calculations do not start with the assumption of identical initial $^{87}Sr/^{86}Sr$ ratios for the Earth and Moon.

Our model age results are presented in Fig. 3 for the four aforementioned impact models and show that only for the canonical impact no Rb-Sr age is obtained. This is consistent with results from an earlier study (Borg et al., 2022) and stems from the fact that in the canonical model the Moon predominantly consists of impactor material (Canup and Asphaug, 2001) and that, therefore, the initial Sr isotope compositions of the Earth and Moon are in most cases quite different. By contrast, in both the fast-spinning Earth (Cuk and Stewart, 2012) and the half Earths models (Canup, 2012), the $^{87}Rb/^{86}Sr$ of the BSE and the initial $^{87}Sr/^{86}Sr$ of the Moon are reproduced only for a relatively narrow range of Moon formation ages of 4.503±0.020 Ga (or 64±20 Ma after solar system formation) and 4.502±0.020 Ga (or 65±20 Ma after solar system formation), respectively. This is because in the fast-spinning Earth scenario, the Moon predominantly consists of proto-Earth material (Cuk and Stewart, 2012). Therefore, the initial Sr isotopic composition of the Moon provides a good proxy for that of the proto-Earth at the time of the impact, which, because Theia is quite small in this scenario, in turn is approximately the initial $^{87}Sr/^{86}Sr$ of Earth. Conversely, in the half Earths model (Canup, 2012), the Moon and Earth are produced from approximately the same mixtures of Theia and proto-Earth material, such that again the initial Sr isotopic composition of the Moon is essentially that of the Earth. Consequently, although these two giant impact models do not assume isotopic equilibration between the Earth and the Moon, they nevertheless predict very similar (but not necessarily identical) initial Sr isotopic compositions for the Earth and the Moon.

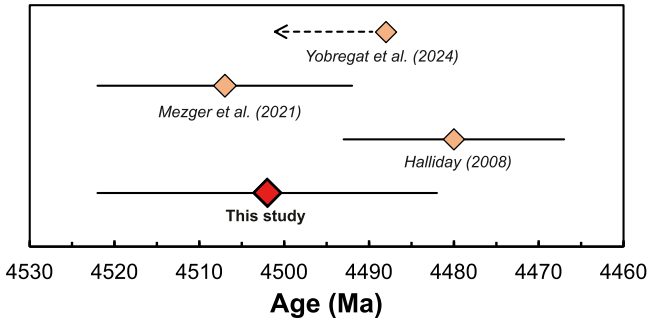

Fig. 4. Comparison of Rb-Sr model ages from different studies. Note that all prior studies assumed post-giant impact Earth-Moon equilibration, whereas this study also considered Moon formation models without equilibration (for details see text). The good agreement among the Rb-Sr ages is partly coincidence, as discussed in the main text.

4.2.3. How well does the Rb-Sr system date the Moon?

Our calculations show that only the canonical impact model does *not* allow to determine a Rb-Sr model age for the formation of the Moon. To account for the Earth-Moon isotopic similarity, this impact scenario requires proto-Earth and Theia to have had the same nucleosynthetic isotope compositions, implying that both formed from the same precursor materials. However, dynamical models of planet formation predict that Earth accreted material from different areas of the accretion disk, and so, given the range of isotopic compositions observed among meteorites and planets, it appears unlikely that proto-Earth and Theia had exactly the same isotopic compositions (e.g., Canup et al., 2023; Pahlevan and Stevenson, 2007), although this possibility is difficult to exclude entirely (e.g., Dauphas et al., 2014). Another argument that is

often cited in favor of post-giant impact Earth-Moon equilibration is the similarity of the ^{182}W isotope signatures of the BSE and the Moon (Kruijer et al., 2015; Kruijer and Kleine, 2017), which is unexpected given that ^{182}W variations record the accretion and core formation histories of Theia and the proto-Earth, which were likely different (Fischer et al., 2021; Kruijer and Kleine, 2017). Although the Moon carries a small ^{182}W excess relative to the present-day BSE (Kruijer et al., 2015; Touboul et al., 2015), this ^{182}W excess can partly or wholly be accounted for by late accretion (i.e. post-core formation addition of material to the mantles of the Earth and Moon), and appears to be smaller than the ^{182}W excess expected in the canonical model of lunar origin (Fischer et al., 2021; Kruijer and Kleine, 2017). As such, the canonical model appears to provide the least realistic scenario to account for the isotopic similarity of the Earth and Moon and, as such, also not for the Rb-Sr isotope evolution of the Earth-Moon system. By contrast, other giant impact models that more readily account for the isotopic similarity of the Earth and Moon provide a consistent Rb-Sr model age for the formation of the Moon, suggesting the Moon formed at 4.502 ±0.020 Ga, or 65±20 Ma after solar system formation.

This Moon formation age is consistent with the occurrence of lunar zircons with crystallization ages of ~4.45–4.42 Ga (Grange et al., 2011; Greer et al., 2023; Meyer et al., 1996; Nemchin et al., 2009, 2008; Taylor et al., 2009; Zhang et al., 2021b) and a Lu-Hf zircon model age for KREEP formation of ~4.43 Ga (Dauphas et al., 2025), all of which are younger than the Rb-Sr age of the Moon. This Moon formation age is also consistent with predictions of recent dynamical models of terrestrial planet formation. While the timing of the last giant impact in these models varies [e.g., from 20 to 180 Ma (Woo et al., 2024)], there is an inverse correlation between the time of the last giant impact and the mass of late-accreted material added to the Earth afterwards (i.e. the late veneer). Since the mass of the late veneer on Earth is known from the abundances of highly siderophile elements in Earth's mantle (Walker, 2009), the correlation of giant impact time with the late-accreted mass can be used to infer the predicted time of the Moon-forming impact for a given set of planet formation simulations. This approach was first used by Jacobson et al. (2014), who inferred an age of the Moon 95±32 Ma after solar system formation, based on a series of 'Grand Tack' simulations. Using the same approach, more recent planet formation models, in which terrestrial planet formation started from a ring of planetesimals at ~1 AU, infer a Moon formation time of ~30–80 Ma after solar system formation (Woo et al., 2024). Thus, the Rb-Sr age for Moon formation 65 ±20 Ma after solar system formation is consistent with predictions from the late-accreted mass on Earth and the dynamics of terrestrial planet formation (Fig. 5).

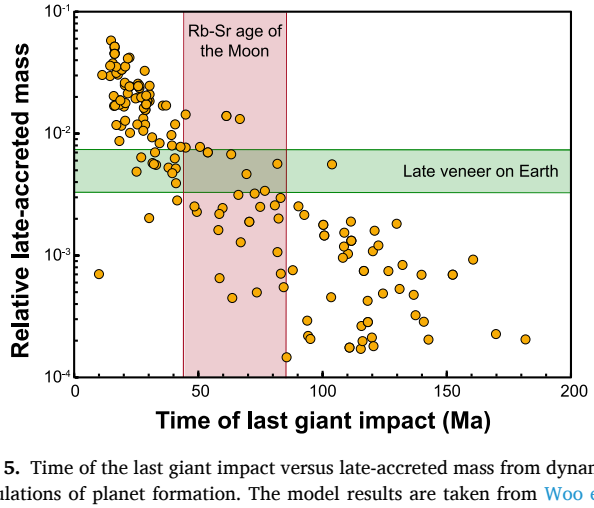

Fig. 5. Time of the last giant impact versus late-accreted mass from dynamical simulations of planet formation. The model results are taken from Woo et al. (2024). The horizontal bar indicates the late-accreted mass on Earth as inferred from the abundances of highly siderophile elements in the Bulk Silicate Earth (Walker, 2009). The vertical bar indicates the Rb-Sr model age of this study and shows excellent agreement with the model predictions.

4.3. Ages of FANs and their link to the lunar magma ocean

Although the Rb-Sr data of this study provide no precise absolute ages for the investigated FANs, the common initial ^{87}Sr/^{86}Sr ratios of the five aforementioned FANs can nevertheless be used to assess a maximum age difference among them. The initial ^{87}Sr/^{86}Sr ratios of these five FANs vary by no more than ±4.8 ppm (as given by the 2 s.d. of their mean ^{87}Sr/^{86}Sr), which in a reservoir characterized by the bulk lunar ^{87}Rb/^{86}Sr of 0.018 corresponds to a time difference of ~14 Ma. Consequently, provided these FANs crystallized from a melt with the bulk lunar ^{87}Rb/^{86}Sr, their common initial ^{87}Sr/^{86}Sr indicates they formed within at most ~28 Ma of each other at ~4.36 Ga (the age of FAN 60025). Since this FAN age is ~150 Ma younger than the Moon's formation age inferred in this study, it does not seem to date the original crystallization of the FANs, which is thought to have started soon after the Moon's formation. As pointed out earlier, the ~4.36 Ga age overlaps with model ages for the mare basalt and KREEP sources, indicating that at this time large parts of the Moon had been in isotopic equilibrium (e.g., Borg et al., 2019; Borg and Carlson, 2023). Consequently, the ~4.36 Ga of FANs is unlikely to reflect unrepresentative sampling or continuous recycling of earlier-formed crust in a long-lived magma ocean. Instead, it more likely reflects a global event, which based on the results of this study, occurred ~150 Ma after the Moon's formation. Based on a prominent ~4.33 Ga age peak among lunar zircons, Barboni et al. (2024) proposed that large-scale re-melting of the Moon occurred at about this time and was likely related to formation of the South-Pole Aitken basin. However, Nimmo et al. (2024) showed that this event is unlikely to have led to the observed global resetting of lunar ages. These authors instead proposed that tidal heating during the Moon's passage through the Laplace plane transition led to a short period of global re-melting at ~4.35 Ga, which reset most lunar ages except those of a few zircons. These authors also showed that heating caused by the continuous intrusion of melt into the pre-existing anorthositic crust led to resetting of ages recorded in crustal materials, consistent with our observation of homogeneous ages among the FANs.

4.4. An emerging chronology of the early Moon

The results of this study, together with those of three recent studies (Barboni et al., 2024; Dauphas et al., 2025; Nimmo et al., 2024), lead to an emerging chronology of the early Moon as follows (Fig. 6). A giant impact formed the Moon at 65±20 Ma, as evident from the consistent Rb-Sr model ages presented here and the relation of late-accreted mass with recent dynamical models (Woo et al., 2024, Fig. 5). This was followed by formation and crystallization of the LMO, which, as is evident from the ages and Lu-Hf systematics of the oldest lunar zircons, reached near-complete solidification ~70 Ma after the Moon's formation (Dauphas et al., 2025). Another ~80 Ma later the Moon underwent a global re-melting event, which was likely triggered by tidal heating and reset all lunar whole-rock ages (Nimmo et al., 2024).

5. Conclusions

New Rb-Sr isotopic data for five lunar ferroan anorthosites provide an initial ^{87}Sr/^{86}Sr of 0.6990608±0.0000005 (2s.e.) for the Moon at 4.360±0.003 Ga. To assess under which circumstances this lunar initial ^{87}Sr/^{86}Sr can be used to determine the Moon's formation time, we modeled the Rb-Sr isotopic evolution of the proto-Earth and Theia. For models in which the isotopic homogeneity of the Earth and Moon reflects either (*i*) post-giant impact equilibration, (*ii*) a Moon consisting predominantly of proto-Earth material, or (*iii*) similar proportions of Theia and proto-Earth materials in the Earth and Moon, we consistenly find a Rb-Sr age of 4.502 ± 0.020 Ga, or 65 ± 20 Ma after solar system formation. By contrast, no Rb-Sr age for the Moon's formation can be

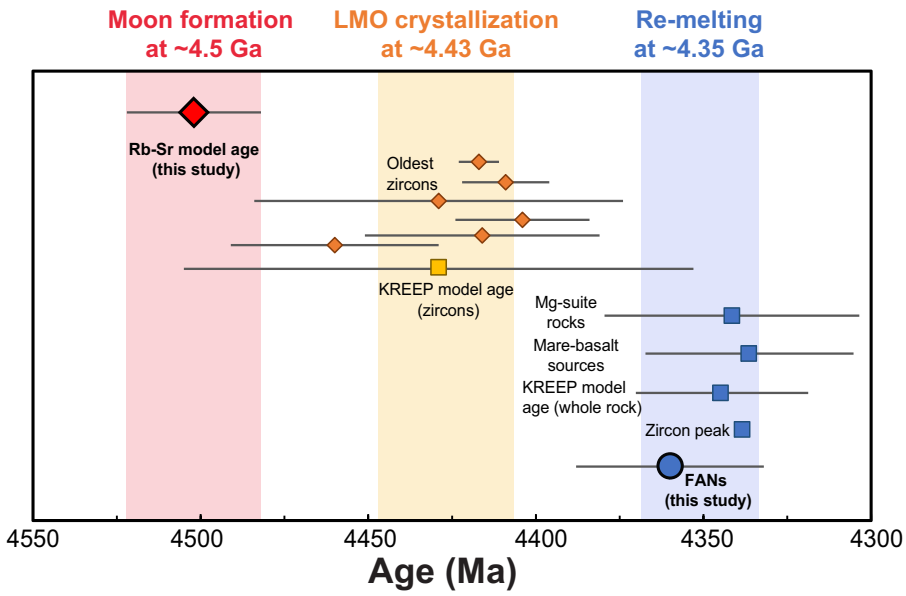

Fig. 6. Chronology of the early Moon with resolved time differences between formation of the Moon as determined by the Rb-Sr system, crystallization of the LMO as inferred from lunar zircons, and a global re-melting event as revealed by lunar whole-rock ages. For literature references of ages see text. Note that only the Lu-Hf zircon model age for KREEP from Dauphas et al. (2025) is shown, because these authors revised earlier results from Barboni et al. (2017).

determined in the canonical model. Formation of the Moon at ~4.5 Ga is consistent with predictions of recent models of terrestrial planet formation, with the occurrence of lunar zircons having crystallization ages of ~4.45–4.42 Ga, and with the most recent Lu-Hf model age of ~4.43 Ga for the end of lunar magma ocean crystallization. From these age constraints a consistent chronology of distinct events in early lunar evolution starts to emerge, suggesting that the lunar magma ocean was near-completely solidified ~70 Ma after the Moon's formation, while a global re-melting event, possibly related to tidal heating, occurred ~80 Ma later and reset all lunar whole-rock ages to ~4.35 Ga, including the FANs of this study.

Data availability statement

All data needed to evaluate the conclusions in the paper are present in the paper and/or the Supplementary Materials.

CRediT authorship contribution statement

Jonas M. Schneider: Writing – review & editing, Writing – original draft, Visualization, Software, Methodology, Investigation, Formal analysis, Data curation, Conceptualization. **Thorsten Kleine:** Writing – review & editing, Supervision, Resources, Project administration, Funding acquisition, Formal analysis, Conceptualization.

Declaration of competing interest

The authors declare that they have no known competing financial interests or personal relationships that could have appeared to influence the work reported in this paper.

Acknowledgements

We thank CAPTEM, NASA and Ryan Zeigler for providing the Apollo lunar samples for this study, and Erik Scherer (University of Münster) for providing the Rb-Sr spike. We thank Olivier Mousis for efficient editorial handling and Richard Carlson and an anonymous reviewer for constructive comments that greatly improved the manuscript.

Funding

This work was funded by the Deutsche Forschungsgemeinschaft (DFG, German Research Foundation) (Project- ID 263649064-TRR170) and the European Research Council Advanced Grant Holy Earth (grant No. 101019380).

Supplementary materials

Supplementary material associated with this article can be found, in the online version, at doi:10.1016/j.epsl.2025.119592.

Data availability

Data will be made available on request.

References

Amelin, Y., 2008. U–Pb ages of angrites. Geochim. Cosmochim. Acta 72, 221–232. https://doi.org/10.1016/j.gca.2007.09.034.

Barboni, M., Boehnke, P., Keller, B., Kohl, I.E., Schoene, B., Young, E.D., McKeegan, K.D., 2017. Early formation of the Moon 4.51 billion years ago. Sci. Adv. 3, e1602365. https://doi.org/10.1126/sciadv.1602365.

Barboni, M., Szymanowski, D., Schoene, B., Dauphas, N., Zhang, Z.J., Chen, X., McKeegan, K.D., 2024. High-precision U-Pb zircon dating identifies a major magmatic event on the Moon at 4.338 Ga. Sci. Adv. 10, eadn9871. https://doi.org/10.1126/sciadv.adn9871.

Borg, L.E., Brennecka, G.A., Kruijer, T.S., 2022. The origin of volatile elements in the Earth–Moon system. Proc. Natl. Acad. Sci. U.S.A 119, e2115726119. https://doi.org/10.1073/pnas.2115726119.

Borg, L.E., Carlson, R.W., 2023. The evolving chronology of moon formation. Annu Rev. Earth. Planet. Sci. 51, 25–52. https://doi.org/10.1146/annurev-earth-031621-060538.

Borg, L.E., Connelly, J.N., Boyet, M., Carlson, R.W., 2011. Chronological evidence that the Moon is either young or did not have a global magma ocean. Nature 477, 70–U150. https://doi.org/10.1038/nature10328.

Borg, L.E., Gaffney, A.M., Kruijer, T.S., Marks, N.A., Sio, C.K., Wimpenny, J., 2019. Isotopic evidence for a young lunar magma ocean. Earth. Planet. Sci. Lett. 523, 115706. https://doi.org/10.1016/j.epsl.2019.07.008.

Borg, L.E., Gaffney, A.M., Shearer, C.K., 2015. A review of lunar chronology revealing a preponderance of 4.34–4.37 Ga ages. Meteorit Planet. Scien. 50, 715–732. https://doi.org/10.1111/maps.12373.

Bottke, W.F., Vokrouhlický, D., Marchi, S., Swindle, T., Scott, E.R.D., Weirich, J.R., Levison, H., 2015. Dating the Moon-forming impact event with asteroidal meteorites. Science (1979) 348, 321–323. https://doi.org/10.1126/science.aaa0602.

Burkhardt, C., Kleine, T., Oberli, F., Pack, A., Bourdon, B., Wieler, R., 2011. Molybdenum isotope anomalies in meteorites: constraints on solar nebula evolution and origin of the Earth. Earth. Planet. Sci. Lett. 312, 390–400. https://doi.org/10.1016/j.epsl.2011.10.010.

Cameron, A.G.W., Ward, W.R., 1976. The Origin of the Moon. Present. Lunar Planet. Sci. Conf. 120.

Canup, R.M., 2012. Forming a moon with an earth-like composition via a giant impact. Science 338, 1052–1055. https://doi.org/10.1126/science.1226073.

Canup, R.M., Asphaug, E., 2001. Origin of the Moon in a giant impact near the end of the Earth's formation. Nature 412, 708–712.

Canup, R.M., Righter, K., Dauphas, N., Pahlevan, K., Ćuk, M., Lock, S.J., Stewart, S.T., Salmon, J., Rufu, R., Nakajima, M., Magna, T., 2023. Origin of the moon. Rev. Mineral. Geochem. 89, 53–102. https://doi.org/10.2138/rmg.2023.89.02.

Canup, R.M., Visscher, C., Salmon, J., Fegley Jr, B., 2015. Lunar volatile depletion due to incomplete accretion within an impact-generated disk. Nat. Geosci. 8, 918–921. https://doi.org/10.1038/ngeo2574.

Carlson, R.W., Lugmair, G.W., 1988. The age of ferroan anorthosite 60025: oldest crust on a young Moon? Earth. Planet. Sci. Lett. 90, 119–130.

Charlier, B.L.A., Tissot, F.L.H., Vollstaedt, H., Dauphas, N., Wilson, C.J.N., Marquez, R.T., 2021. Survival of presolar p -nuclide carriers in the nebula revealed by stepwise leaching of Allende refractory inclusions. Sci. Adv. 7, eabf6222. https://doi.org/10.1126/sciadv.abf6222.

Charnoz, S., Sossi, P.A., Lee, Y.-N., Siebert, J., Hyodo, R., Allibert, L., Pignatale, F.C., Landeau, M., Oza, A.V., Moynier, F., 2021. Tidal pull of the Earth strips the proto-Moon of its volatiles. Icarus 364, 114451. https://doi.org/10.1016/j.icarus.2021.114451.

Cuk, M., Stewart, S.T., 2012. Making the moon from a fast-spinning Earth: a giant impact followed by resonant despinning. Science 338, 1047–1052. https://doi.org/10.1126/science.1225542.

Dauphas, N., Burkhardt, C., Warren, P.H., Fang-Zhen, T., 2014. Geochemical arguments for an Earth-like Moon-forming impactor. Philos. Trans. A. Math. Phys. Eng. Sci. 372, 20130244. https://doi.org/10.1098/rsta.2013.0244.

Dauphas, N., Zhang, Z.J., Chen, X., Barboni, M., Szymanowski, D., Schoene, B., Leya, I., McKeegan, K.D., 2025. Completion of lunar magma ocean solidification at 4.43 Ga. Proc. Natl. Acad. Sci. 122, e2413802121. https://doi.org/10.1073/pnas.2413802121.

Elardo, S.M., Draper, D.S., Shearer, C.K., 2011. Lunar Magma Ocean crystallization revisited: bulk composition, early cumulate mineralogy, and the source regions of the highlands Mg-suite. Geochim. Cosmochim. Acta 75, 3024–3045. https://doi.org/10.1016/j.gca.2011.02.033.

Fischer, R.A., Zube, N.G., Nimmo, F., 2021. The origin of the Moon's Earth-like tungsten isotopic composition from dynamical and geochemical modeling. Nat. Commun. 12, 35. https://doi.org/10.1038/s41467-020-20266-1.

Gaffney, A.M., Borg, L.E., 2014. A young solidification age for the lunar magma ocean. Geochim. Cosmochim. Acta 140, 227–240. https://doi.org/10.1016/j.gca.2014.05.028.

Grange, M.L., Nemchin, A.A., Timms, N., Pidgeon, R.T., Meyer, C., 2011. Complex magmatic and impact history prior to 4.1 Ga recorded in zircon from Apollo 17 South Massif aphanitic breccia 73235. Geochim. Cosmochim. Acta 75, 2213–2232. https://doi.org/10.1016/j.gca.2011.01.036.

Greer, J., Zhang, B., Isheim, D., Seidman, D.N., Bouvier, A., Heck, P.R., 2023. 4.46 Ga zircons anchor chronology of lunar magma ocean. Geochem. Persp. Let 27, 49–53. https://doi.org/10.7185/geochemlet.2334.

Halliday, A.N., 2008. A young Moon-forming giant impact at 70-110 million years accompanied by late-stage mixing, core formation and degassing of the Earth. Phil. Trans. Roy. Soc. Lond. 366, 4163–4181.

Hans, U., Kleine, T., Bourdon, B., 2013. Rb-Sr chronology of volatile depletion in differentiated pro-toplanets: BABI, ADOR and ALL revisited. Earth. Planet. Sci. Lett. 374, 204–214. https://doi.org/10.1016/j.epsl.2013.05.029.

Hartmann, W.K., Davis, D.R., 1975. Satellite-sized planetesimals and lunar origin. Icarus 24, 504–515. https://doi.org/10.1016/0019-1035(75)90070-6.

Jacobson, S.A., Morbidelli, A., Raymond, S.N., O'Brien, D.P., Walsh, K.J., Rubie, D.C., 2014. Highly siderophile elements in Earth's mantle as a clock for the Moon-forming impact. Nature 508, 84. https://doi.org/10.1038/nature13172.

Kleine, T., Münker, C., Mezger, K., Palme, H., 2002. Rapid accretion and early core formation on asteroids and the terrestrial planets from Hf–W chronometry. Nature 418, 952–955. https://doi.org/10.1038/nature00982.

Kleine, T., Hans, U., Irving, A.J., Bourdon, B., 2012. Chronology of the angrite parent body and implications for core formation in protoplanets. Geochim. Cosmochim. Acta 84, 186–203. https://doi.org/10.1016/j.gca.2012.01.032.

Kruijer, T.S., Kleine, T., 2017. Tungsten isotopes and the origin of the Moon. Earth. Planet. Sci. Lett. 475, 15–24. https://doi.org/10.1016/j.epsl.2017.07.021.

Kruijer, T.S., Kleine, T., Fischer-Gödde, M., Sprung, P., 2015. Lunar tungsten isotopic evidence for the late veneer. Nature 520, 534–537. https://doi.org/10.1038/nature14360.

Lock, S.J., Stewart, S.T., Petaev, M.I., Leinhardt, Z., Mace, M.T., Jacobsen, S.B., Cuk, M., 2018. The origin of the moon within a terrestrial synestia. J. Geophys. Res. 123, 910–951. https://doi.org/10.1002/2017JE005333.

Maurice, M., Tosi, N., Schwinger, S., Breuer, D., Kleine, T., 2020. A long-lived magma ocean on a young Moon. Sci. Adv. 6. https://doi.org/10.1126/sciadv.aba8949 eaba8949.

Meyer, C., Williams, I.S., Compston, W., 1996. Uranium-lead ages for lunar zircons: evidence for a prolonged period of granophyre formation from 4.32 to 3.88 Ga. Meteorit. Planet. Sci. 31, 370–387. https://doi.org/10.1111/j.1945-5100.1996.tb02075.x.

Mezger, K., Maltese, A., Vollstaedt, H., 2021. Accretion and differentiation of early planetary bodies as recorded in the composition of the silicate Earth. Icarus 365, 114497. https://doi.org/10.1016/j.icarus.2021.114497.

Michaut, C., Neufeld, J.A., 2022. Formation of the lunar primary crust from a long-lived slushy magma ocean. Geophys. Res. Lett. 49. https://doi.org/10.1029/2021GL095408 e2021GL095408.

Moynier, F., Day, J.M.D., Okui, W., Yokoyama, T., Bouvier, A., Walker, R.J., Podosek, F.A., 2012. Planetary-scale strontium isotopic heterogeneity and the age of volatile depletion of early solar system materials. Astrophys. J. 758, 45.

Nebel, O., Mezger, K., Scherer, E.E., Münker, C., 2005. High precision determinations of 87Rb/85Rb in geologic materials by MC-ICP-MS. Int. J. Mass Spectrom. 246, 10–18. https://doi.org/10.1016/J.IJMS.2005.08.003.

Nemchin, A., Timms, N., Pidgeon, R., Geisler, T., Reddy, S., Meyer, C., 2009. Timing of crystallization of the lunar magma ocean constrained by the oldest zircon. Nat. Geosc 2, 133–136. https://doi.org/10.1038/ngeo417.

Nemchin, A.A., Pidgeon, R.T., Whitehouse, M.J., Vaughan, J.P., Meyer, C., 2008. SIMS U–Pb study of zircon from Apollo 14 and 17 breccias: implications for the evolution of lunar KREEP. Geochim. Cosmochim. Acta 72, 668–689. https://doi.org/10.1016/j.gca.2007.11.009.

Nimmo, F., Kleine, T., 2015. Early differentiation and core formation. The Early Earth. American Geophysical Union (AGU), pp. 83–102. https://doi.org/10.1002/9781118860359.ch5.

Nimmo, F., Kleine, T., Morbidelli, A., 2024. Tidally driven remelting around 4.35 billion years ago indicates the Moon is old. Nature 636, 598–602. https://doi.org/10.1038/s41586-024-08231-0.

Pahlevan, K., Stevenson, D.J., 2007. Equilibration in the aftermath of the lunar-forming giant impact. Earth. Planet. Sci. Lett. 262, 438–449. https://doi.org/10.1016/j.epsl.2007.07.055.

Papanastassiou, D.A., Wasserburg, G.J., 1978. Strontium isotopic anomalies in the Allende meteorite. Geophys. Res. Lett. 5, 595–598.

Schneider, J.M., Burkhardt, C., Kleine, T., 2023. Distribution of s-, r-, and p-process nuclides in the early Solar system inferred from Sr isotope anomalies in meteorites. ApJL 952. https://doi.org/10.3847/2041-8213/ace187. L25.

Schneider, J.M., Kleine, T., 2024. Effects of Faraday cup deterioration on Sr and Cr isotope analyses by thermal ionization mass spectrometry. J. Anal. At. Spectrom. Acccept.

Smith, J.V., Anderson, A.T., Newton, R.C., Olsen, E.J., Wyllie, P.J., 1970. A petrologic model for the moon based on petrogenesis, experimental petrology, and physical properties. J. Geol. 78, 381–405. https://doi.org/10.1086/627537.

Snyder, G.A., Taylor, L.A., Neal, C.R., 1992. A chemical model for generating the source of mare basalts: combined equilibrium and fractional crystallization of the lunar magmasphere. Geochim. Cosmochim. Acta 56, 3809–3823.

Taylor, D.J., McKeegan, K.D., Harrison, T.M., 2009. Lu–Hf zircon evidence for rapid lunar differentiation. Earth. Planet. Sci. Lett. 279, 157–164. https://doi.org/10.1016/j.epsl.2008.12.030.

Tera, F., Papanastassiou, D.A., Wasserburg, G.J., 1974. Isotopic evidence for a terminal lunar cataclysm. Earth. Planet. Sci. Lett. 22, 1–21. https://doi.org/10.1016/0012-821X(74)90059-4.

Tissot, F.L.H., Dauphas, N., Grove, T.L., 2017. Distinct 238U/235U ratios and REE patterns in plutonic and volcanic angrites: geochronologic implications and evidence for U isotope fractionation during magmatic processes. Geochim. Cosmochim. Acta 213, 593–617. https://doi.org/10.1016/j.gca.2017.06.045.

Touboul, M., Puchtel, I.S., Walker, R.J., 2015. Tungsten isotopic evidence for disproportional late accretion to the Earth and Moon. Nature 520, 530–533. https://doi.org/10.1038/nature14355.

Walker, R.J., 2009. Highly siderophile elements in the Earth, Moon and Mars: update and implications for planetary accretion and differentiation. Chem Erde-Geochem 69, 101–125. https://doi.org/10.1016/j.chemer.2008.10.001.

Warren, P.H., 1985. The magma ocean concept and lunar evolution. Annu. Rev. Earth Planet. Sci. Lett. 13, 201–240.

Warren, P.H., Wasson, J.T., 1979. The origin of KREEP. Rev. Geophys. Space Phys 17, 73–88.

Wetherill, G.W., 1975. Late heavy bombardment of the moon and terrestrial planets. Proc. 6th Lunar Planet. Sci. Conf 2, 1539–1561.

Wolf, R., Anders, E., 1980. Moon and Earth : compositional differences inferred from siderophiles, volatiles, and alkalis in basalts. Geochim. Cosmochim. Acta 44, 2111–2124. https://doi.org/10.1016/0016-7037(80)90208-2.

Woo, J.M.Y., Nesvorný, D., Scora, J., Morbidelli, A., 2024. Terrestrial planet formation from a ring: long-term simulations accounting for the giant planet instability. Icarus 417, 116109. https://doi.org/10.1016/j.icarus.2024.116109.

Wood, J.A., Dickey, J.S., Marvin, U.B., Powell, B.N., 1970. Lunar anorthosites. Science 167, 602–604. https://doi.org/10.1126/science.167.3918.602.

Yobregat, E., Fitoussi, C., Bourdon, B., 2024. Rb-Sr constraints on the age of Moon formation. Icarus 420, 116164. https://doi.org/10.1016/j.icarus.2024.116164.

Zhang, B., Lin, Y., Moser, D.E., Hao, J., Liu, Y., Zhang, J., Barker, I.R., Li, Q., Shieh, S.R., Bouvier, A., 2021a. Radiogenic Pb mobilization induced by shock metamorphism of zircons in the Apollo 72255 Civet Cat norite clast. Geochim. Cosmochim. Acta 302, 175–192. https://doi.org/10.1016/j.gca.2021.03.012.

Zhang, B., Lin, Y., Moser, D.E., Warren, P.H., Hao, J., Barker, I.R., Shieh, S.R., Bouvier, A., 2021b. Timing of lunar Mg-suite magmatism constrained by SIMS U-Pb dating of Apollo norite 78238. Earth. Planet. Sci. Lett. 569, 117046. https://doi.org/10.1016/j.epsl.2021.117046.